2E-13

Proceedings of Symposium on Ultrasonic Electronics, Vol. 31 (2010) pp. 437-438
6-8 December, 2010

Measurement of Two-Dimensional Heart Wall Motion for Evaluation of Myocardial Contraction and Relaxation at High Temporal Resolution

心筋収縮弛緩特性計測を目指した心臓壁 2 次元運動の高時間分解能計測

Yasunori Honjo[1†], Hideyuki Hasegawa[1, 2] and Hiroshi Kanai[2, 1] ([1]Graduate School of Biomedical Eng., Tohoku Univ.; [2]Graduate School of Eng., Tohoku Univ.)
本庄 泰徳[1‡], 長谷川 英之[1, 2], 金井 浩[2, 1] ([1]東北大 医工; [2]東北大 工)

1. Introduction

In recent years, there have been many studies on the measurement of myocardial strain or strain rate, and techniques for measuring them have been developed[1,2]. However, a mechanism of the transitions between myocardial contraction and relaxation was unclear. Some transitions of heart wall motion rapidly occur during a short period of about 10 ms[3]. Under such rapid motion of heart, two-dimensional (2-D) speckle tracking techniques[2] may fail to estimate the heart wall motion accurately at a low frame rate because it leads to significant changes in echo patterns. Therefore, to track the heart wall motion accuracy, a frame rate is required more than 1000 Hz (1 ms).

In our previous study, 2-D displacement of the heart wall was estimated by employing the interpolated normalized cross-correlation function[4] between RF echoes obtained by the parallel beam forming[5]. In the present study, 2-D myocardial strain rate was measured by a speckle tracking method (2-D tracking) so that the myocardial function could be measured at a high frame rate.

2. Principle

The axial velocity $v_a(i, j; n)$ and lateral velocity $v_l(i, j; n)$ between the n-th and $n+\Delta N_F$ -th frames at a point (i, j) (i: lateral, j: axial positions) in a heart wall are given by the determined lateral shift Δm_n and axial shift k_n, which maximize the interpolated normalized cross-correlation function, respectively, as follows:

$$v_a(i,j;n)=\frac{c_0\cdot\Delta k_n}{2f_s\cdot\Delta N_F\cdot\Delta T}\quad[\text{mm/s}],\qquad(1)$$

$$v_l(i,j;n)=\frac{\Delta m_n\cdot\delta l}{\Delta N_F\cdot\Delta T}\quad[\text{mm/s}],\qquad(2)$$

where c_0 and δl are the sound speed and the lateral spacing $\delta l = 2d\cdot\sin\delta\theta$ ($\delta\theta$: angular interval of beams) at depth d, respectively.

We introduced the strain rate to evaluate how the thickness of each layer changes with respect to time. As shown in **Fig. 1**, strain rate in the axial and lateral directions, $S_a(i, j; n)$ and $S_l(i, j; n)$, of the i-th lateral and j-th axial layers are given by

$$S_a(i,j;n)=\frac{v_a(i,j+1;n)-v_a(i,j;n)}{\Delta D}\quad[(\text{m/s})/\text{m}],\qquad(3)$$

$$S_l(i,j;n)=\frac{v_l(i+1,j;n)-v_l(i,j;n)}{\Delta\Theta}\quad[(\text{m/s})/\text{m}].\qquad(4)$$

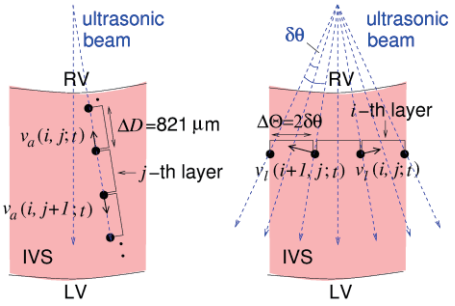

Fig. 1: Method of assigning layers in the axial direction (a) and lateral direction (b) in IVS.

3. Basic Experimental Results

3.1 Experimental System

As illustrated in **Fig. 2**, in this experiment, strain rate of a phantom due to the change in the internal pressure, which was applied by a flow pump, was measured. The homogeneous cylindrical phantom was made from silicone rubber whose thickness was about 2 mm. RF data were acquired using a 3.75 MHz sector-type probe of ultrasonic diagnostic equipment (Aloka α-10). The sampling frequency of the RF signal was 15 MHz. The frame rate and angular interval of beams δθ were 1024 Hz and 0.375 degree, respectively.

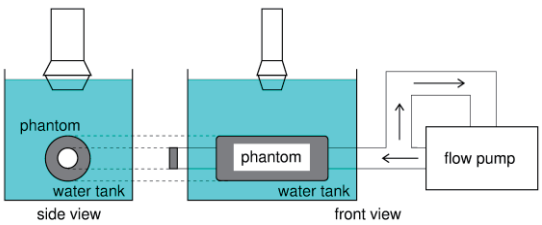

Fig. 2: Schematic of system for basic experiment.

3.2 Experimental Result

As shown in **Fig. 3**, the displacements (a) in a

E-mail: honjo@us.ecei.tohoku.ac.jp
(hasegawa, kanai)@ecei.tohoku.ac.jp

region in the lateral and axial directions and strain rates in the axial and lateral directions of the regions colored in Fig. 3(b) and 3(c), respectively, were estimated by 2-D tracking. After 0.2 s from the beginning of pulsation of the pump (at (1)~(3) in Fig. 3(a)), the wall thickness of the phantom decreased both in the axial and lateral directions. On the other hand, after 0.75 s from the beginning of pulsation of the pump (at (4)~(6) in Fig. 3(a)), the wall thickness of the phantom increased both in the axial and lateral directions.

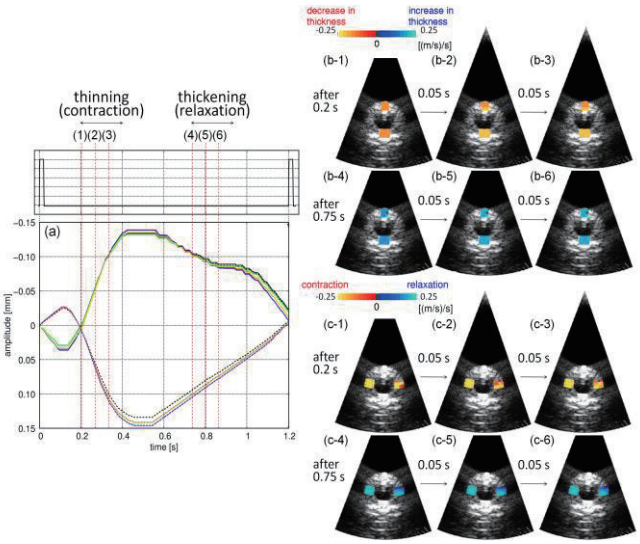

Fig. 3: (a) Displacement of the phantom. Distributions of the strain rate at four different times in the axial (b) and lateral (c) directions.

4. *In Vivo* Experimental Results

As shown in **Fig. 4(a)**, the velocities in a region in the IVS (45 yellow points in Fig. 4(a)) were estimated by 2-D tracking. The size of a correlation kernel was set at (13.5×8.3) mm[4]. Figures 4(b-1) and 4(b-2) show the velocities of the IVS at each point in the axial and lateral direction obtained by the 2-D correlation function, respectively.

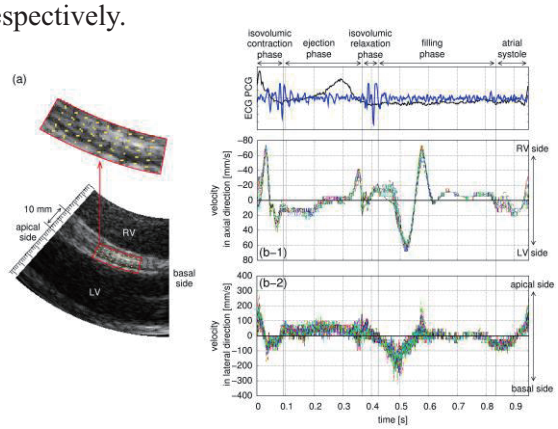

Fig. 4: (a) Acquisition area of the RF echoes from the longitudinal-axis view. (b) Velocities at the yellow points in the axial (1) and lateral (2) direction.

Figures 5(b) and 5(c) show the distribution of strain rates at every 10 ms in the axial and lateral directions at the beginning of the ejection phase. The strain rate in the axial direction is perpendicular to that in lateral direction. Therefore, myocardial contraction and relaxation (in the lateral direction) in the IVS correspond to increase and decrease in thickness in the axial direction, respectively[1, 3]. This phenomenon of strain rates obtained by 2-D tracking was in good agreement with those relationships and myocardial systole.

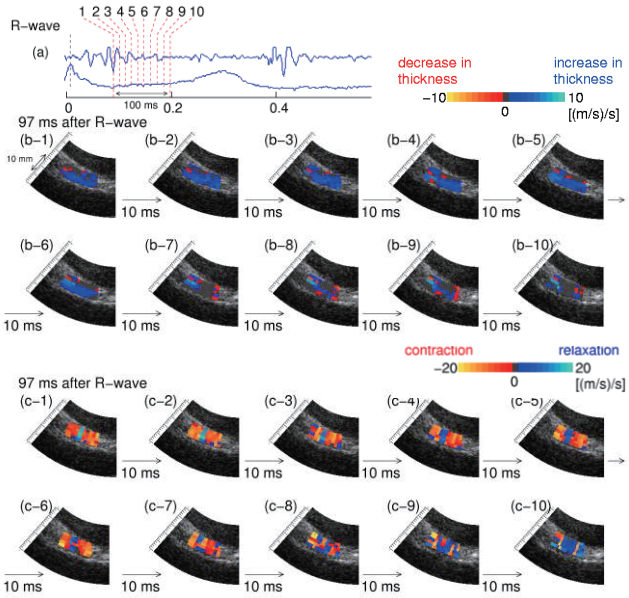

Fig. 5: (a) Electrocardiogram and phonocardiogram. Distributions of the strain rate at ten different times during the ejection phase in the axial (b) and lateral (c) directions.

5. Conclusion

Regional myocardial velocity and strain rate were measured at high temporal resolutions. As shown in Fig. 5, *in vivo* experimental results show the possibility of this method for measurement of 2-D heart motion to assess the regional myocardial contraction and relaxation at a high temporal resolution.

References

1. H. Kanai, Y. Koiwa, Y. Saito, I. Susukida and M. Tanaka: Jpn. J. Appl. Phys. **38** (1999) 3403.
2. L. N. Bohs, B. J. Geiman, M.E. Anderson, S. C.Gebhart and G. E. Trahey: Ultrasonics **38** (2000) 369.
3. Y. Yoshiara, H. Hasegawa, H. Kanai and M. Tanaka: Jpn. J. Appl. Phys. **46** (2007) 4889.
4. Y. Honjo, H. Hasegawa and H. Kanai: Jpn. J. Appl. Phys. **49** (2010) 07HF14.
5. H. Hasegawa and H. Kanai: IEEE. Trans. UFFC. **55** (2008) 2626.